Periodic Orbits and Equilibria in Glass Models for Gene Regulatory Networks

Igor Zinovik, Yury Chebiryak, and Daniel Kroening

***Abstract*—Glass models are frequently used to model gene regulatory networks. A distinct feature of the Glass model is that its dynamics can be formalized as paths through multi-dimensional binary hypercubes. In this paper, we report a broad range of results about Glass models that have been obtained by computing the binary codes that correspond to the hypercube paths. Specifically, we propose algorithmic methods for the synthesis of specific Glass networks based on these codes. In contrast to existing work, bi-periodic networks and networks possessing both stable equilibria and periodic trajectories are considered. The robustness of the attractor is also addressed, which gives rise to hypercube paths with nondominated nodes and double coils. These paths correspond to novel combinatorial problems, for which initial experimental results are presented. Finally, a classification of Glass networks with respect to their corresponding gene interaction graphs for three genes is presented.**

***Index Terms*—Circuit codes, dominating codes, gene regulatory networks, hypercube, induced cycle, snake-in-the-box codes, wiring diagram.**

I. Introduction

ANALYSIS of the dynamics and regulation of gene expressions has become one of the most important areas in Systems Biology. Microarray chip techniques generate an endless stream of data, which can shed light on these cell dynamics at the molecular level, a task that requires appropriate analysis algorithms. The complexity of genetic regulatory networks requires formal models and automated analysis algorithms.

The state-of-the-art models for the regulation of gene expressions include Bayesian networks, Boolean networks, nonlinear ordinary differential equations, and piecewise-linear differential equations. The origin of many of these models can be traced back to the work of R. Thomas and S. Kauffman, who suggested several approaches for the formalization of regulatory networks as dynamic systems evolving over time. Extensive reviews of modeling and simulation of genetic networks can be found in [3], [4].

Manuscript received May 05, 2009. Current version published February 24, 2010. The work was supported in part by ETH Research Grant TH-19 06-3. The material in this paper was presented in part at the 7th Australia–New Zealand Mathematics Convention, Christchurch, New Zealand, December 11, 2008.

I. Zinovik is with LTNT Laboratory of Thermodynamics in Emerging Technologies, ETH Zurich, ML J38, 8092 Zurich, Switzerland (e-mail: izinovik@ethz.ch).

Y. Chebiryak is with the Computer Systems Institute, ETH Zurich, RZ H15, 8092 Zurich, Switzerland (e-mail: yury.chebiryak@inf.ethz.ch).

D. Kroening is with the Computing Laboratory, Oxford University, Wolfson Building, Parks Road, Oxford OX1 3QD, U.K. (e-mail: kroening@comlab.ox.ac.uk).

Communicated by O. Milenkovic, Associate Guest Editor for the Special Issue on Molecular Biology and Neuroscience.

Digital Object Identifier 10.1109/TIT.2009.2037078

We focus on models that utilize differential equation systems, as they are based on a well-developed formalism for the chemical kinetics. These models capture the concentrations of cell proteins as functions of time. We furthermore focus on a special class of piecewise-linear differential equations (PLDE), which was proposed by Glass and Kauffman as an approximative model for the network dynamics in the context of gene regulation [5], [6]. *Glass PLDE* are not intended to model the chemical kinetics of the proteins precisely; they capture only the basics of the chemical reactions and represent the dynamics of gene expressions qualitatively. In return, the relative simplicity of the model enables many analytical results, which elucidate many properties of the gene regulatory system.

This style of modeling exploits a distinctive feature of gene regulatory systems: the interactions are characterized by a very *localized coupling* of the state variables, unlike complex couplings found in control and electronic circuit problems. The models are formulated as *hybrid systems* in which the switch-like behavior of genes is approximated by discrete steps, while the other state variables still change continuously over time. These models have been used for the analysis of gene regulatory networks [7]–[10] and neural networks [11], [12].

A distinct feature of the Glass model is that its dynamics can be described using paths through multi-dimensional binary hypercubes, that is, binary codes. This embeds reasoning about Glass models into the rich context of information theory. The scope of this paper is the development of computational methods for the analysis of the Glass PLDE based on an analysis of these codes, and their application for reasoning about the features of the model that are biologically relevant.

A. Contribution

The core contribution of this paper is an analytical framework for Glass PLDE that is based on the analysis of codes on binary hypercubes. The hypercube codes are computed by means of modern propositional satisfiability (SAT) solvers [13], [14]. The utility of our framework is demonstrated by the following three results.

1) In most of the existing literature, the discussion of the dynamics of Glass PLDE is restricted to either the case of a single stable periodic orbit or multiple equilibria. As our first contribution, we address instances of Glass networks of two types: a) with stable bi-periodicity and b) with co-existent equilibrium and stable periodic trajectory. Our reduction to hypercube paths enabled a full classification of the six-dimensional networks with a cyclic attractor with respect to the number of equilibrium states co-existent with the attractor. We have also synthesized instances of all networks with double attractors up to dimension seven and

TABLE I
GLOSSARY OF TERMS

Phase space	An n-dimensional (locally compact and metric) space that is defined by all possible valuations of the functions that satisfy the ODE system is called the *phase space* of the system. In the Glass model, the phase space represents the space of all possible values of concentrations of the proteins regulated by the gene network.
Phase space trajectory (orbit)	A set of points of the phase space that represent valuations of the solution functions for a specified time interval with a given initial point is called the *phase trajectory*. In the Glass model, the trajectory depicts the dynamics of the network protein concentrations over a given time interval starting from an initial state.
Phase flow	A set of phase trajectories that originate in a subspace of the phase space of the system. Alternatively, the term refers to a parametric transformation of the phase space, mapping it to itself where the parameter is a time instant. In the Glass model, the phase flow can be represented as a path on hypercube; the path defines a sequence of valuations of the gene expressions where the expressions are given as a binary labeling of the hypercube nodes.
Attractor	A phase trajectory that serves as an attracting set for the trajectories originating in a vicinity of the attractor. Single-point attractors are called *equilibrium points* of the system. In the Glass model, equilibrium points represent stable states of the gene network where gene expressions remain constant over time.
Periodic orbit (trajectory)	A closed-loop phase trajectory corresponding to a periodic solution of the system. Glass introduced the term *cyclic attractor* for periodic attractors with an extended basin of attraction. They simulate stable periodic biological processes such as cell division, where protein concentrations and gene expressions are periodic functions of time.
Multiperiodicity	The property of ODE systems of possessing more than one periodic orbit. In the biological context, such systems serve as models of the gene networks with the potential to regulate more than one cell division pattern.

present new upper bounds on the total length of the attractors.

2) In contrast to the models with continuous ODE, the wiring schemes of PLDE and their connection to the system dynamics have not been studied systematically. We have extended our SAT-based approach to the construction of Glass networks that correspond to a given wiring scheme. We also present a classification of the transition diagrams of the networks with respect to the wiring schemes of the models. To the best of our knowledge, it is the first classification of this kind for the Glass PLDE.
3) Sufficient conditions for periodic orbits in Glass networks require the computation of eigenvalues and eigenvectors of the matrix that specifies the Poincaré return map of the phase flow [15]. Based on those criteria, we have developed an algebraic method for the synthesis of Glass networks with periodic orbits along given cycles in the transition diagram. As an exemplar, we construct a set of three-dimensional Glass networks with periodic orbits for the given transition diagrams. Finally, we suggest two conjectures about the transition diagrams, which can be seen as colloraries of conjectures for ODE systems [16].

We emphasize that the connection between the cyclic codes and the Glass PLDE is independent of the specific way the codes are obtained. In particular, our exhaustive computation is likely not sufficient for many biological systems, which can easily contain hundreds of genes. A promising direction is therefore the construction of longer codes (or proofs of the nonexistence of specific longer codes) by means of recursion schemes, e.g., those described by Tanner graphs [17], [18].

B. Outline

We begin with a short, formal introduction into the Glass PLDE model. In Section III, we discuss Glass networks that are appropriate to model cell division. The corresponding hypercube paths give rise to two novel combinatorial problems. In Section IV, we discuss wiring diagrams for Glass PLDE, and examine conjectures for models with continuous ODE in this context. In Section V, we suggest an algebraic method for the construction of Glass PLDE with periodic orbits that avoids the complications connected with numerical methods.

C. Related Work

Various approaches to the search for the equilibrium states in a variety of gene regulatory networks have been presented in the literature. In PLDE systems, the search for the equilibrium states and for periodic trajectories in the models of networks is known to be computationally demanding due to the combinatorial explosion of the size of the search space [19]. In case of PLDE with equilibrium states, a scalable search algorithm has been proposed recently by de Jong and Page [20]. Their method reduces the search to a first-order-logic satisfiability problem and relies on the heuristics implemented in the state-of-the-art solvers for satisfiability modulo theories (SMT).

The existing efforts to deduce fully defined dynamic models of gene regulatory systems are limited by the lack of experimental data on the kinetic constants of the biochemical reactions. Nevertheless, the models can be used to infer qualitative information about the *interaction* of the genes. Interaction is one of the most important properties of gene regulatory systems and is usually presented in the form of a *wiring scheme*. A wiring scheme is a directed graph that specifies *inhibiting* and *activating* interactions between the genes. In systems biology, the connection between qualitative dynamics of ODE-based models and their wiring schemes has been a research focus since the pioneering work of Thomas and Kauffman [21]. The results have been summarized as conjectures that link the equilibria and the periodic behavior of autonomous ODE to inhibiting and activating patterns of wiring schemes [16].

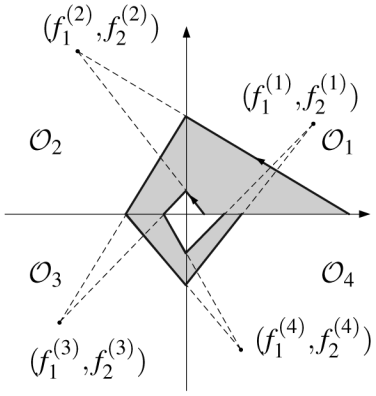

Fig. 1. A 2D phase flow.

II. An Introduction to the Glass PLDE Model

This section provides a brief introduction into the Glass PLDE Model, its applications in Systems Biology, and explains the connection to cyclic binary codes. Table I contains a glossary with the most important terms.

A. Glass PLDE and Their Dynamics

The Glass PLDE Model [15] tracks the concentration of the products of n genes. We denote the concentration of the product of gene i by x_i. The switch-like behavior of genes is modeled with the help of thresholds for these concentrations, which induces a partitioning of the PLDE phase space into a set of n-dimensional boxes. The dynamics of the system are given by a separate ODE for each of the boxes

$$\dot{x}_i = \mu_i - \gamma_i x_i \quad \text{for } 1 \le i \le n$$

where μ_i is a constant production rate and γ_i is the rate of decay of protein i.

If the model of the gene activity is restricted to on/off expressions and the decay rates are identical for all reactions, the PLDE system is called a Glass model. Using appropriate scaling of the variables, the Glass PLDE can be transformed into the system

$$\dot{y}_i = F_i(\tilde{y}_1, \ldots, \tilde{y}_n) - y_i \quad \text{for } 1 \le i \le n,$$

where $\tilde{y}_i = 0$ if $y_i < 0$ and $\tilde{y}_i = 1$ if $y_i > 0$ [15]. These equations describe a network in which all thresholds are equal to 0 and the decay rate is 1. The partitioning by the thresholds coincides with the orthants $\mathcal{O}_k$, $k \in \{1, 2, 3, \ldots, 2^n\}$ of the phase space.

The trajectory of the PLDE in each partition is always a straight line; the flow in orthant $\mathcal{O}_k$ is defined by its *focal point* $\boldsymbol{f}^{(k)} = (f_1^{(k)}, f_2^{(k)}, \ldots, f_n^{(k)}) \in \mathbb{R}^n$ where $f_i^{(k)} = F_i(\tilde{y}_1, \tilde{y}_2, \ldots, \tilde{y}_n)|_{\mathcal{O}_k}$. Thus, the Glass network can be fully specified by a choice of focal points $\boldsymbol{f}^{(1)}, \ldots, \boldsymbol{f}^{(2^n)}$. Fig. 1 illustrates a phase flow with two trajectories in a two-dimensional Glass network.

The state transition diagram is an overapproximation of the phase flow. It is depicted by an n-dimensional cube with directed edges. Each orthant of the phase space is mapped to a node of the n-cube, and each common boundary of the orthants corresponds to an edge of the cube. This edge is directed according to the direction of the phase flow across the boundary [22]. The state transition diagram for a three-dimensional Glass network is shown in Fig. 2.

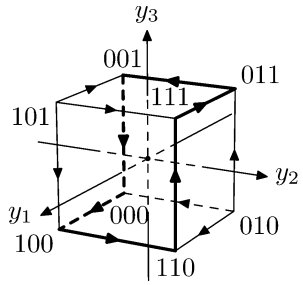

Fig. 2. A 3D transition diagram.

The nodes of the n-cube are labeled by vectors of n binary variables $(\tilde{y}_1, \tilde{y}_2, \ldots, \tilde{y}_n)$, which define a valuation of the network interaction functions F_i. Periodic trajectories of a network correspond to closed cycles in the transition graph (as an example, consider the thick path in Fig. 2). This connection enables reasoning about the phase flow in the Glass networks by examining the set of paths on the n-cube, a problem of independent importance in coding theory. In particular, the existance of a cycle in the transition diagram is a necessary condition for the existence of periodic orbits in Glass networks.

B. Cyclic Attactors

The global phase flow in Glass networks can be quite complex. Oscillations towards equilibrium states, cycles and limit cycles may occur when the linear parts of the trajectories are connected continuously over sequences of orthants [15], [19], [22], [23]. Numerical simulations [22], [24] indicate that for dimensions greater than 4, Glass networks may exhibit aperiodic and chaotic behavior.

Studies of the periodic solutions for Glass models show that there are networks that possess a special type of stable limit cycles: the flow between the orthants along these cycles is unambiguous, i.e., for each orthant along the cycle, all trajectories must go to the same successor.[1] Networks with stable cycles of this kind are called networks with *cyclic attractors* [22]. We formalize this concept as a property of the state transition diagram.

Definition 1 (Cyclic Attractor): A cycle in the state transition diagram is called a *cyclic attractor* if a) it is a chord-free simple cycle in the n-cube,[2] and b) all edges adjacent to the cycle are directed towards the cycle nodes.

As an example, the cycle shown in Fig. 2 is the cyclic attractor.

In information theory, an attractor is known as cyclic *snake-in-the-box code* in a hypercube [25]. The search for snakes is motivated by the theory of error-correcting codes (as the vertices of a solution to the snake or coil in the box problems can be used as a Gray code that can detect single-bit

[1] In other words, the basin of attraction of the periodic trajectory is composed of all orthants spanned by the trajectory.

[2] Every edge in the graph that joins two vertices of the cycle is an edge of this cycle.

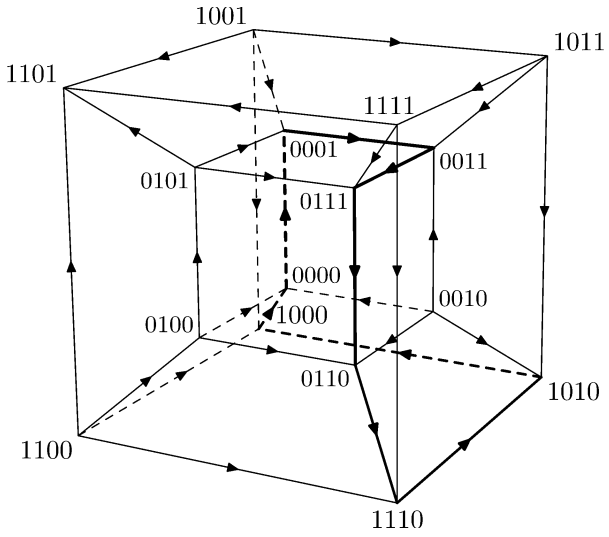

Fig. 3. An induced cycle in the 4-cube. The cycle *shuns* node 1101.

errors). Such a code can also be seen as an instance of a *circuit code* of spread 2 (circuit codes are useful for correcting and limiting errors in analog-to-digital conversion, see [26], [27]).

III. Glass Networks With Complex Attracting Sets

A. Glass Networks for Cell Division

Models for gene regulatory networks with equilibrium states and stable limit cycles are of special interest in Systems Biology, as these models simulate cell differentiation processes and explain the variability of cell types [21], [28]. Cell division cycles require models with periodic orbits. A normal development of the cell division should eventually stop with a tissue consisting of a finite number of cells, thus suggesting that the model has to have multiple stable (equilibrium) states as well.

We use the vulval development of *C. elegans* as an example. This development process exhibits a series of cell divisions with 22 nuclei finally formed. The cell division process reveals dynamics of a complex reactive system that includes at least four different molecular signaling pathways [29].

We discuss the implications of these observations on the corresponding Glass model. The state of each of the four signaling pathways is described by valuation of a Boolean variable, and the transition diagram is a four-dimensional cube. The diagram has to contain both a cyclic attractor (representing the switching of gene expressions during the cycles of cell division) and a node that specifies the final state of the system. All edges of this final node have to be directed inwards to ensure that the phase flow has a stable equilibrium in the corresponding orthant of the phase space of the Glass PLDE.

We formalize the existence of a stable equilibrium as a property of the state transition diagram. Observe that the Hamming distance between the equilibrium node and the nodes of the cyclic attractors has to be greater than one.[3] We say that such a node is *nondominated* or *shunned* by the cycle [2]. A formal definition of this property follows.

[3]Otherwise, the orientation of at least one of the edges of the equilibrium node will be inconsistent with the definition of a cyclic attractor (Def. 1).

Definition 2: The cycle $I_0 \dots I_{L-1}$ *shuns* node W of the n-cube if W is not adjacent to any node of the cycle

$$\forall j \in \{0, \dots, L-1\}. \quad d_H^n(I_j, W) > 1 \tag{1}$$

where $d_H^n(a, b)$ denotes the Hamming distance between nodes a and b of the n-cube.

An example of a four-dimensional transition diagram with a cyclic attractor and an equilibrium node is given in Fig. 3. The orthants for the focal points of the PLDE are defined by the orientation of the diagram edges. A way to ensure the existence of a periodic orbit is to require focal coordinates of 1 or -1 [30].[4]

Nondominated nodes in state transition diagrams have further implications on the dynamics of the Glass PLDE.[5] The classification of the cyclic attractors with respect to the number of nondominated nodes is therefore highly desirable.

Propositional SAT Encoding of Induced Cycles: We employ a propositional satisfiability (SAT) solver in order to obtain the required codes. We provide a formalization of the encoding.[6] We use $n \cdot L$ Boolean variables $I_j[k]$, where $0 \leq j < L$ and $0 \leq k < n$, to encode the coordinates of an induced cycle of length L in the n-cube. The variable $I_j[k]$ denotes the kth coordinate of the jth node. In order to form a cycle in an n-cube, consecutive nodes of the sequence must have Hamming distance 1, including the last and the first

$$\varphi_{\text{cycle}} := \left(\bigwedge\nolimits_{i=0}^{L-2} d_H^n(I_i, I_{i+1}) = 1 \right) \wedge d_H^n(I_{L-1}, I_0) = 1.$$

The Hamming distance d_H is encoded efficiently using *once-twice* chains, as described in [31]. In brief, a once-twice chain identifies differences between two code words up to some position j based on 1) comparing them at position j, and 2) recursively comparing their prefixes up to position $j-1$.

To make the cycle induced, we eliminate chords as follows:

$$\varphi_{\text{chord-free}} := \bigwedge_{\substack{0 \leq i < j < L, \\ d_C^n(i,j) \geq 2}} d_H^n(I_i, I_j) \geq 2$$

where $d_C^n(k, m) = \min\{|k-m|, L-|k-m|\}$. This also ensures that the nodes along the cycle are pairwise distinct. In practice, the formula $\varphi_{\text{chord-free}}$ can be optimized by eliminating half of its clauses, using an argument presented in [32].

The conjunction of these constraints is an encoding of induced cycles:

$$\varphi_{\text{IC}} := \varphi_{\text{cycle}} \wedge \varphi_{\text{chord-free}}.$$

[4]The Glass networks with such focal points are called Boolean Glass networks.

[5]For example, the presence of nodes nondominated by the cycle also indicates that the phase flow along the attractor is *robust* to arbitrary perturbations of the coefficients that define the equations in the orthant corresponding to the node. This robustness implies that the periodic behavior of the gene network will not be affected by the (likely unknown) protein production rate in any state corresponding to the nondominated node.

[6]The details of the setup of the propositional SAT solver are beyond the scope of this article. We refer the interested reader to [2].

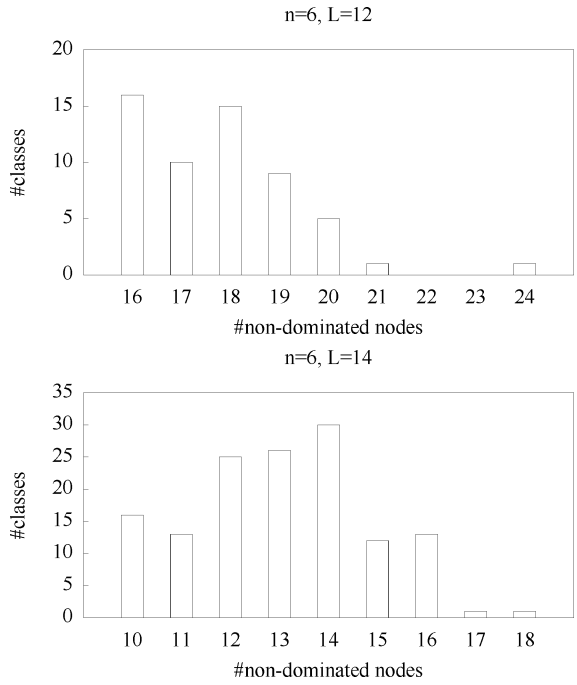

Fig. 4. The classification of cyclic attractors in six-dimensional hypercubes with a given length L with respect to the number of nondominated nodes.

We encode the property that a cycle $I_0 \dots I_{L-1}$ shuns nodes $u_0, \dots, u_{S-1}$ by requiring the distance of the nodes to the cycle to be at least 2

$$\varphi_{\text{shunned}} := \bigwedge_{i=0}^{S-1} \bigwedge_{j=0}^{L-1} d_H^n(u_i, I_j) \geq 2.$$

We combine this with the condition that the nodes are distinct,

$$\varphi_{\text{distinct}} := \bigwedge_{0 \leq i < j < S} d_H^n(u_i, u_j) \geq 1$$

to obtain an encoding of induced cycles with at least S shunned nodes:

$$\varphi_{\text{ICS}} := \varphi_{IC} \wedge \varphi_{\text{shunned}} \wedge \varphi_{\text{distinct}}. \tag{2}$$

Every solution of (2) corresponds to an induced cycle of length L in the n-cube with at least S shunned nodes. We aim at the cycles with a maximum S. We obtain these codes by starting with *cube-dominating* induced cycles, i.e., with $S = 0$, and increasing S until the SAT solver reports unsatisfiability.[7]

The results for the known instances of attractors in dimension 7 indicate that some cyclic attractors with the longest period may shun up to three nodes. Table II summarizes our results for the longest attractors and the attractors with a maximum number of nondominated nodes. The partitioning of the equivalence classes of cyclic attractors with respect to the number of nondominated nodes they admit is presented in Table III and Fig. 4.

[7]As the range of values for S for which (2) is satisfiable is contiguous, a binary search strategy is also possible, using a heuristically determined initial value for S.

TABLE II
THE NUMBER OF NONDOMINATED NODES FOR THE LONGEST CYCLIC ATTRACTORS

dimension n	max length L	#non-dominated nodes
3	6	0
4	8	{0, 1}
5	14	0
6	26	0
7	48	{0, 1, 2, 3, ?}

TABLE III
THE NUMBER OF EQUIVALENCE CLASSES OF CYCLIC ATTRACTORS

dimension n	length L	#non-dominated nodes	#cycles
5	10	0	0
		1	0
		2	3
		3	3
		4	3
		5	0
		6	1
5	12	0	2
		1	0
		2	2
		3	0
		4	1
5	14	0	3
6	12	16	16
		17	10
		18	15
		19	9
		20	5
		21	1
		22	0
		23	0
		24	1
6	14	10	16
		11	13
		12	25
		13	26
		14	30
		15	12
		16	13
		17	1
		18	1
6	16	0	1
		1	0
		2	1
		3	1
		4	13
		5	14
		6	44
		7	60
		8	108
		9	105
		10	111
		11	53
		12	34
		13	7
		14	8
		15	1
		16	2

In Fig. 4, we also report the results of this classification for two new equivalence classes of six-dimensional transition diagrams. We have previously reported a classification of the induced cycles of length 16, which exceeds the maximal length of the induced cycles in cubes of dimension five [33]. However, it is possible to construct induced cycles shorter the maximal length in previous dimensions, which nevertheless cannot be found in the cubes of lower dimensions. The minimum length of such a cycle in a cube of dimension n cannot be less than $2n$, because

TABLE IV
THE CUBES WITH TWO CYCLIC ATTRACTORS

Dimension n	max length L	First attractor			Second attractor		
		length	start node	coordinate sequence	length	start node	coordinate sequence
4	8	4	1111	4242	4	0010	4242
5	14	6	01010	153153	6	00100	513513
6	26	20	001110	26536156254356251245	4	000010	2626
7	48	24	0011000	124165716417347562574563	24	1111111	312517234523761571374562

the cycle has to traverse all dimensions of the cube. In dimensions greater than 6, an example of such a cycle can be given by the following sequence of node coordinates switching along the cycle: $(1,\ldots,n,1\ldots,n)$.[8]

B. Multiperiodic Glass Networks

An important feature of models of gene networks with chaotic dynamics is *multiperiodicity* [16]. The transition diagrams of such multiperiodic systems have to contain multiple cycles. If a gene network exhibits dynamics with multiple stable periodic orbits, a Glass PLDE with multiple cyclic attractors may be a suitable model. The transition diagrams of these Glass networks have to possess multiple induced cycles.

We have extended our propositional encoding of single induced cycles [1], [33] in order to perform a search for multiple cycles. We have identified all hypercubes with two cyclic attractors up to dimension seven (Table IV). The combined length of two attractors was found to be less than the maximum length of the single attractor in the cubes up to dimension six. In dimension seven, the combined length reaches the maximum length of the single cycle. An exhaustive search was feasible up to dimension six, which implies that the results in the table are indeed tight: there are no cubes with a combined length of the two cycles exceeding those that are shown in the table.

The above definitions for complex attracting sets in the Glass networks give a rise to two novel combinatorial problems related to paths in hypercubes. The two problems can be formulated as follows:

1) What is maximum number of nondominated nodes in hypercubes with an induced cycle of given length L?
2) What is the combined length of multiple induced cycles in a cube of given dimension n?

The co-existence of a longest cyclic attractor and a nondominated node in the same model suggests that during cell division, the gene network may traverse a maximum possible number of different states before switching to the final equilibrium. The combined length of the induced cycles is an upper bound on the number of states of the multiperiodic system.

IV. TRANSITION DIAGRAMS AND WIRING SCHEMES

A. Background on Wiring Schemes

Wiring schemes or *interaction graphs* are the most common way to present information on the interaction between genes.

[8]It is easy to see that a cycle with such coordinate sequence of length $L = 2n$ is indeed an induced cycle, as the sequence satisfies the criterium given in [6]: 1) Each coordinate in the sequence must appear an even number of times. 2) For any sequence of length shorter than L, at least one coordinate must appear an odd number of times. 3) Every sequence of consecutive digits of length I, where I is an odd integer $3 \leq I \leq L-3$, must contain at least 3 coordinates that appear an odd number of times.

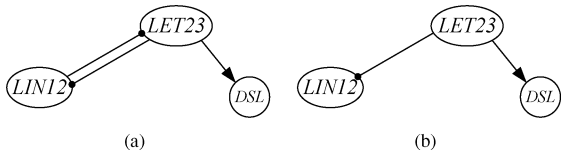

Fig. 5. Two candidate wiring schemes for the vulval development of *C. elegans*, derived from [37].

Formally, a wiring scheme is an oriented and labeled graph whose vertices represent the variables of the system. The graph specifies *inhibiting* and *activating* interactions between the genes. We write $g_1 \longrightarrow g_2$ if g_1 activates g_2, and $g_1 \multimap g_2$ if g_1 inhibits g_2.

The wiring scheme can be interpreted as a description of the information flow between the components. For the case of Glass PLDE, the wiring scheme describes relations between the individual bits of the binary codes that represent the dynamics of the PLDE. Bits (genes) can be independent, and when information is exchanged, this information flow may be cyclic or cycle-free. In the context of Glass PLDE, a wiring scheme therefore serves a similar purpose as a Tanner graph [17]. The wiring scheme is often deduced by solving an inverse problem for a chosen model of the system. The Glass PLDE can serve as the underlying model if the experimental data series are sufficiently long [34]. Nevertheless, a systematic study of the interaction graphs related to PLDE is rarely presented in the literature.[9] In contrast, the wiring schemes of ODE with continuous coefficients are widely studied and well understood (see [16] for further references). The results can be formulated in the form of conjectures that link equilibria and periodic behavior of autonomous ODE to inhibiting and activating patterns of the gene interaction.

B. A Comparison of ODE Versus PLDE

The gene interaction for ODE with continuous coefficients is defined by the signs of the elements of Jacobian matrix $||J||$ of the system [16]. If $J_{ij} > (<)0$, then gene j activates (inhibits) gene i. The edges of the wiring scheme are labeled by the sign of the corresponding Jacobian element. The wiring scheme is said to have a positive (negative) *circuit* in a point $\mathbf{x}$ of the state space if a product of J_{ij} with cyclical permutation of indexes (i,j) is positive (negative).

The conjectures about the circuits of the wiring schemes have been formulated as follows:

[9]To the best of our knowledge, the only study addressing the link between the phase flow of PLDE and their wiring scheme is presented in [35], [36]. The result presented in [35] states that if the wiring scheme is a cycle with one negative interaction, it is always possible to construct a PLDE system with stable periodic orbit. In [36], it was proved that in a subset of PLDE, multistationarity implies existence of positive interactions between the genes.

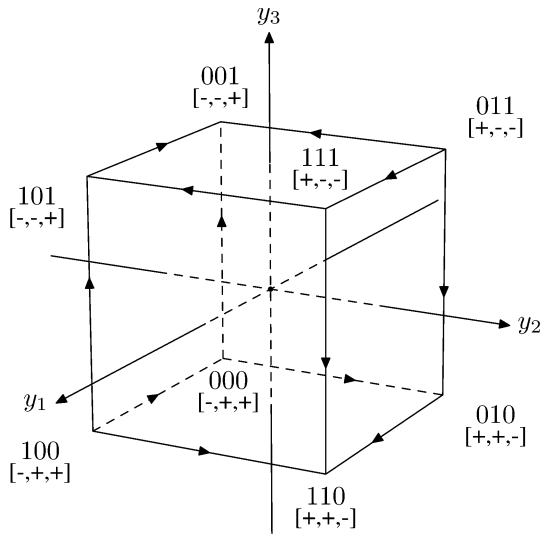

Fig. 6. A unique cube complying to the wiring scheme in Fig. 5(a). Signs of focal points are denoted in brackets. Dimensions 1, 2, and 3 correspond to signaling pathways DSL, LET23, and LIN12, respectively.

1) The presence of a positive circuit (somewhere in the phase space) is a necessary condition for multistationarity.
2) The presence of a negative circuit of length at least two (somewhere in the phase space) is a necessary condition for stable periodicity.

We investigate whether these conjectures are valid in the case of PLDE systems. As a first step, we identify the differences between the modeling of gene interactions in PLDE systems and in ODE with continuous coefficients. In the PLDE, the Jacobian is not defined on the threshold hyperplanes, and thus by definition, $i \longrightarrow j$ implies that an increase of x_i may lead to an increase of the kinetic rate of protein production linked to μ_j at least at some point $\mathbf{x}$ in the state space [35]. If the increase of the concentration leads to a decrease of the kinetic rate, this is depicted as $i \multimap j$. For the Glass PLDE, the definition is consistent with the definition of the schemes for ODE with continuous coefficients, with two noteworthy differences:

1) if the Jacobian-based definition is applied to the Glass PLDE within the coordinate orthants, the wiring scheme will contain self-inhibiting edges at every node of the scheme whereas the definition of the PLDE wiring scheme does not require any self-regulating edges;
2) in contrast to Jacobian-based schemes, which characterize the interactions for a given local point, the PLDE wiring schemes present *all* local interactions on one graph.

To analyze the conjectures above in the context of PLDE, we need a definition of positive (negative) circuits in PLDE wiring schemes that is consistent with the definition for ODE with continuous coefficients and does not require the computation of derivatives. We propose the following definition: a circuit is called positive (negative) if the circuit contains an even (odd) number of inhibiting edges.

We apply our encodings of hypercube paths to check the conjectures for the Glass networks as follows: In Glass networks, multistationarity in the phase flow is equivalent to the presence of two or more equilibrium nodes in the oriented hypercubes. If the hypercubes contain a cyclic attractor, the Glass PLDE admits a stable periodic orbit. Therefore, a classification of the hypercubes with equilibria and attractors with respect to their wiring schemes could possibly provide a counterexample for the conjectures.

It is known that the search over oriented hypercubes is computationally demanding due to the rapid explosion of the search space. For example, in the four dimensional case, the number of the cubes reaches 2^{32} and search is usually performed using random sampling [19]. For our classification, we obtain the set of hypercubes for a given wiring scheme as a solution of a propositional satisfiability problem.

Our encoding is based on a set of independent Boolean variables that define the labels of the nodes and orientations of the edges (the details of the encoding are in the Appendix). These variables are used to introduce a set of dependent Boolean variables that represent the signs of focal points and the interactions between the genes. The dependent variables are defined as functions of the variables for the labels and the orientations according to the definitions of the focal points and the gene interactions. The wiring scheme of interest is encoded as Boolean constraint such that satisfiable assignments identify the transition diagrams of the networks. In the following, we first suggest a number of applications and then discuss the results of a full classification for gene networks with three genes.

C. The Vulval Development of C. Elegans

As an illustrative example, we have identified the transition diagrams of the Glass networks with the wiring schemes that represent the interactions of the genes of *C. elegans* presented in [37]. The vulval development of *C. elegans* is an example of a simple and very well-studied process of cell division, which relies on a relatively small gene regulatory network. The *C. elegans* vulva is developed from a set of precursor cells, which are capable of adopting one of several fates. The adopted fate depends on several intercellular signals that affect the interactions of the genes. The experimental data admits different interpretations of the interactions and a final choice requires additional knowledge about the nature of the interactions. This knowledge can be provided by fixing a suitable model for the regulatory network.

If the Glass model is used to model the interactions, the fates can be seen as equilibrium points of the Glass systems. Consequently, reasoning about the cyclic attractors of the possible Glass models allows us to make a choice between two candidates for the regulatory network.

The literature suggests several alternative possibilities for the gene interactions that explain the formation of the cell patterns with two distinct fates [37]. The two interaction graphs that can be deduced from these diagrams are given in Fig. 5.

We performed a search over all 2^{12} oriented 3D cubes with the following constraints: 1) every edge of the wiring schemes has to appear at least once and 2) no edges except those shown are allowed. The search with our propositional satisfiability encoding of the problem required $7\,s$ (see Table VII in the Appendix for the full results). The search shows that for the scheme in Fig. 5(a), there is only one transition diagram and that it has two equilibrium nodes. This transition diagram is given in Fig. 6. The second wiring scheme (Fig. 5(b)) was found to admit two

TABLE V
ATTRACTORS INDUCING WS WITH VARIABLE EDGES

Dimension	Length	#WS without variable edges	%WS without variable edges	#coils (total)	#WS with variable edges
6	12	57	100	57	0
	14	52	38	137	85
	16	140	25	563	423
	18	142	12	1228	1086
	20	73	7	1032	959
	22	7	1	478	471
	24	4	4	110	106
	26	0	0	4	4
5	10	10	100	10	0
	12	2	40	5	3
	14	0	0	3	3
4	8	3	100	3	0

TABLE VI
HYPERCUBE EDGES, CORRESPONDING CHANGES IN FOCAL POINTS AND INFERRED GENE INTERACTION

Coordinates change		Focal point change				Wiring scheme
$000 \to 100$	(1^+)	$[1,-1,1]$	$\to$	$[1,-1,-1]$	(3^-)	$g_1 \multimap g_3$
$000 \to 001$	(3^+)	$[1,-1,1]$	$\to$	$[1,1,1]$	(2^+)	$g_3 \longrightarrow g_2$
$001 \to 011$	(2^+)	$[1,1,1]$	$\to$	$[-1,1,1]$	(1^-)	$g_2 \multimap g_1$
$001 \to 101$	(1^+)	$[1,1,1]$	$\to$	$[1,1,-1]$	(3^-)	$g_1 \multimap g_3$
$010 \to 000$	(2^-)	$[-1,-1,1]$	$\to$	$[1,-1,1]$	(1^+)	$g_2 \multimap g_1$
$010 \to 011$	(3^+)	$[-1,-1,1]$	$\to$	$[-1,1,1]$	(2^+)	$g_3 \longrightarrow g_2$
$101 \to 100$	(3^-)	$[1,1,-1]$	$\to$	$[1,-1,-1]$	(2^-)	$g_3 \longrightarrow g_2$
$101 \to 111$	(2^+)	$[1,1,-1]$	$\to$	$[-1,1,-1]$	(1^-)	$g_2 \multimap g_1$
$110 \to 100$	(2^-)	$[-1,-1,-1]$	$\to$	$[1,-1,-1]$	(1^+)	$g_2 \multimap g_1$
$110 \to 010$	(1^-)	$[-1,-1,-1]$	$\to$	$[-1,-1,1]$	(3^+)	$g_1 \multimap g_3$
$111 \to 011$	(1^-)	$[-1,1,-1]$	$\to$	$[-1,1,1]$	(3^+)	$g_1 \multimap g_3$
$111 \to 110$	(3^-)	$[-1,1,-1]$	$\to$	$[-1,-1,-1]$	(2^-)	$g_3 \longrightarrow g_2$

oriented cubes, each of which has a single equilibrium node. These results indicate that the cell dynamics of *C. elegans* with its two distinct stationary states cannot be modeled using the second scheme.[10]

D. Wiring Diagrams With Variable Edges

An important property of gene networks is the ability of interaction between two genes to change from inhibition to activation and vice versa, depending on the expressions of the genes [38]. In PLDE systems, the wiring schemes of such networks will contain an edge that has different signs in different nodes of the transition diagram. Following the definition for ODE with continuous coefficients [16], we shall call such edges *variable edges*. The presence or lack of variable edges in a wiring scheme may serve as another classification criterion for transition diagrams.

As an example of such a classification, we have computed how many cyclic attractors induce wiring schemes with variable edges. The variable edges in the schemes were identified using the coordinate sequences of the equivalence classes of the attractors obtained in [33]. The results for the attractors are summarized in Table V and Fig. 7. We found that the relative number of the equivalence classes with variable edges increases with an increasing length of the attractor, and that in dimensions five and six, the wiring schemes of all attractors of maximum period have variable edges. This result implies that in the Glass model, stable periodic orbits of maximum length cannot be described by the wiring schemes without variable edges.[11]

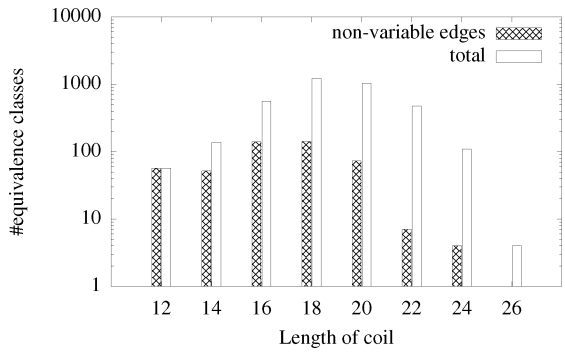

Fig. 7. Classification of coils with respect to variable edges of wiring scheme.

Our satisfiability encoding provides a flexible tool for the synthesis of transition diagrams with prescribed properties for their wiring schemes. As an example, we constructed a four-dimensional oriented cube with an oriented Hamiltonian cycle where the wiring scheme does not contain any variable edges (see Fig. 8).

In order to further evaluate the scalability of our SAT-based search, we have constructed five-dimensional oriented hypercubes that conform to the wiring scheme in Fig. 9. This wiring scheme is adopted from [39] and outlines relationships among

[10]Observe that this conclusion is consistent with the multistationarity conjecture, i.e., the first scheme has the positive circuit $1 \multimap 2 \multimap 1$, which manifests the necessary condition of multistationarity, whereas the second wiring scheme does not have the circuits.

[11]Note that this classification of the attractors is based on the coordinate sequences along the nodes of the attractors. It is possible to construct different transition diagrams with attractors from the same equivalence class in such a way that one of the diagrams induces a wiring scheme without variable edges and the other one will have at least one variable edge.

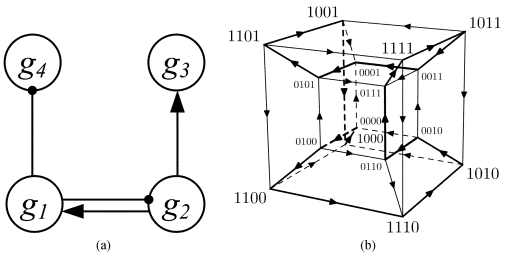

Fig. 8. A sample Boolean Glass network with Hamiltonian path and its wiring scheme. (a) Wiring diagram. (b) Boolean Glass network.

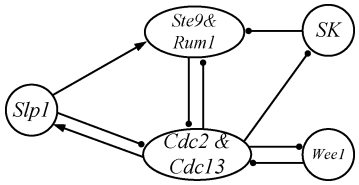

Fig. 9. The wiring diagram of eukariotic cell division [39].

the principal molecular components of the cell cycle engine during the cell division.

Since the scheme models periodic changes of the concentrations of the cell proteins, we have implemented a search for the transition diagrams that possess at least one simple or complex cycle of a prescribed length. We encode the problem as a propositional SAT formula. The encoding leaves the choice of the orientation of the edges to the SAT solver. The orientations are only constrained by the given wiring scheme: their choice depends on the choices of incident edges and restrictions on focal points dictated by a wiring scheme. We restrict the cube to have a cycle of a prescribed length using the encoding of simple cycles by Papadimitriou (see Example 8.1 in [40] for Hamiltonian cycles in arbitrary graphs). This simple cycle may be a part of a complex cycle.

In order to identify how many cycles are in the resulting hypercube, we employ a backtracking algorithm proposed by Szwarcfiter and Lauer [41], which improves the asymptotically fastest algorithm by D. B. Johnson [42]. We identify strongly connected components using Tarjan's algorithm [43]. The results of the computations are summarized in Table VIII (in Appendix C), listing all possible configurations (i.e., the number of complex cycles and equilibria, see also Fig. 10). The results show that the algorithm is able to perform an exhaustive search up to cycle length 32 in less than 16 hours of CPU time.

Fig. 10 and Table VIII (in the Appendix) present results of the run of our algorithm on cubes complying to the scheme in Fig. 9 for all lengths of cycles from 4 to 32.

E. A Full Classification for Networks With Three Genes

In Systems Biology, a classification of the networks in lower dimensions is also desirable, owing to the possibility of elucidating the fundamental links between the system dynamics and the elements of complex gene interactions. In [16], a full classification of the possible dynamics of ODE with continuous coefficients with respect to the wiring schemes is shown for two-gene networks. To the best of our knowledge, there is no report of such a classification for the Glass PLDE model.

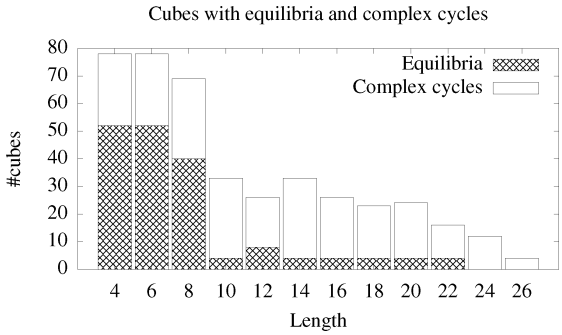

Fig. 10. Hypercubes with complex cycles and equilibria.

As a first step of a comprehensive classification of the Glass networks, we suggest to begin with the analysis of three interacting genes. We have applied our SAT-based search for the synthesis of the transition diagrams for all possible wiring schemes with three nonvariable edges. An exhaustive conditional search was carried out assuming that in all wiring schemes, every edge has to be enforced at least at one node of the transition diagram and that there are no other edges in the scheme except those shown. The schemes and their diagrams are presented in the Appendix. We observe that the full set comprises of 28 wiring schemes that comply with 67 oriented cubes. A total of 15 wiring schemes correspond to a unique oriented cube, and not more than four cubes with the same scheme can be constructed in the set. Furthermore, a total of 24 transition diagrams have simple or complex cycle and 10 among them include cyclic attractors. Single equilibrium nodes were found in 39 cubes, whereas 14 diagrams possess two equilibrium nodes. In those cubes with cyclic attractors and double equilibrium nodes, the wiring schemes have negative or positive circuits, respectively. Since in both cases of the transitions in the diagrams express sufficient conditions for the corresponding dynamics of the Boolean Glass PLDE, we observe that the conjectures described above hold in all Boolean Glass networks with equilibrium nodes and with cyclic attractors.

While the cubes with cyclic attractors ensure the existence of the Glass PLDE with stable periodic orbits along the attractors, periodic phase flow may also exist in the networks without cyclic attractors. In such networks, the analysis of the conjecture about periodic orbits requires an additional step, as the criteria for periodic orbits [15] have to be checked. For example, the wiring schemes $1 \longrightarrow 2 \dashv 3 \dashv 1$ and $1 \longrightarrow 2 \longrightarrow 3 \longrightarrow 1$ constitute positive circuits and are induced by the transition diagrams with simple cycles of length six (see Appendix). The existence of a Glass network with a stable periodic orbit and one of these transition diagrams would be a counterexample for the PLDE-version of the conjecture.

V. Construction of Glass Networks With Periodic Orbits

A. Criteria for Periodic Orbits

The construction of the Glass PLDE with periodic orbits reported in the literature relies on random specification of the focal coordinates [19] and subsequent numerical calculations

TABLE VII
WIRING SCHEMES WITH 3 EDGES ALONG WITH TYPES OF GLASS NETWORKS COMPLYING TO THEM

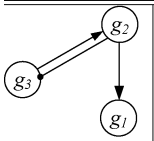 bi-periodicity	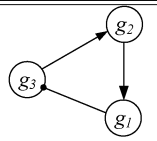 6-attractor	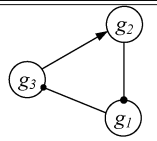 6-coil, 2 equilibria	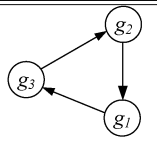 6-coil, 2 equilibria
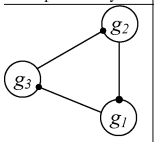 6-attractor	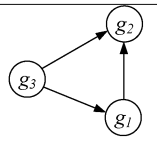 1 equilibrium	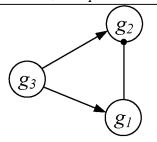 1 equilibrium	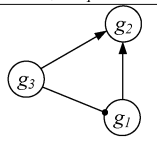 1 equilibrium
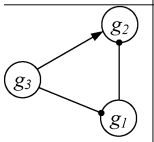 4 cubes with 1 eq.	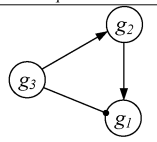 4 cubes with 1 eq.	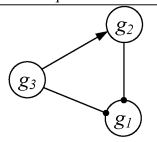 4 cubes with 1 eq.	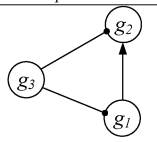 4 cubes with 1 eq.
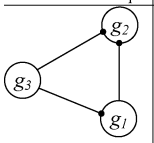 4 cubes with 1 eq.	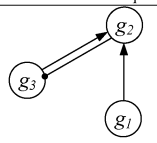 2 cubes with 4-coil + 1 eq., 2 cubes with 4-attractor	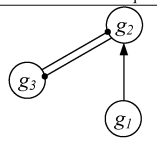 2 cubes with 1 eq., 2 cubes with 2 eq.	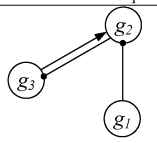 2 cubes with 4-coil + 1 eq., 2 cubes with 4-attractor
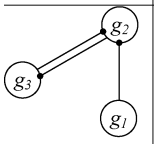 2 cubes with 2 eq. 2 cubes with 1 eq.	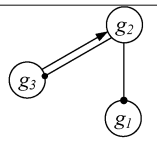 bi-periodicity	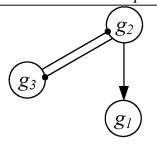 1 cube with 2 eq.	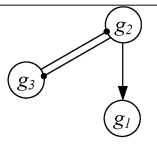 1 cube with 2 eq.
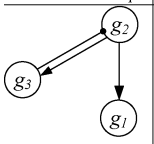 bi-periodicity	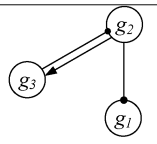 bi-periodicity	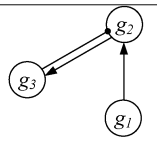 2 cubes with 4-coil + 1 eq., 2 cubes with 4-attractor	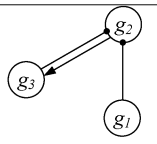 2 cubes with 4-coil + 1 eq., 2 cubes with 4-attractor
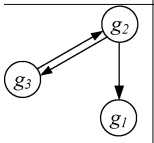 1 cube with 2 eq.	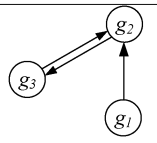 2 cubes with 2 eq., 2 cubes with 1 eq.	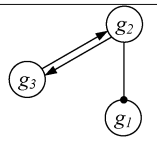 1 cube with 2 eq.	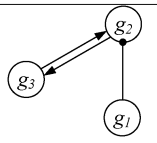 2 cubes with 2 eq., 2 cubes with 1 eq.

that check the criteria [15]. The conclusions based on the calculations are limited by the rounding errors introduced during the numerical procedure. In this final section, we therefore suggest an algebraic method for the construction of Glass PLDE with periodic orbits that avoids the complications connected with numerical methods and the ambiguity of the random choice of the focal points.

In the Glass model, the transition diagrams define only the signs of the focal points of the Glass PLDE but do not specify the phase flow unambiguously. A perturbation of the absolute values of the focal coordinates may lead to a bifurcation between periodic orbits and a flow converging to the origin [1]. If the signs of the focal coordinates are fixed and only absolute values of the coordinates are perturbed, the Glass PLDE will possess the same transition diagram. We exploit this observation to perform synthesis of Glass networks with periodic orbits.

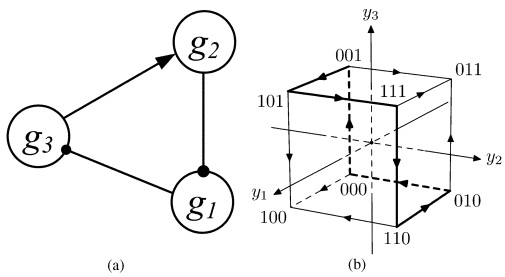

Fig. 11. A wiring scheme with a positive circuit and the unique Boolean Glass network complying to it. The network has a six-coil (bold arrows) and two equilibria (hollow nodes). (a) Wiring diagram. (b) Boolean Glass network.

We assume that the given transition diagram has a cycle that is meant to define a periodic phase flow. Our construction is based on the criteria for periodic flow in the Glass PLDE [15]. Let

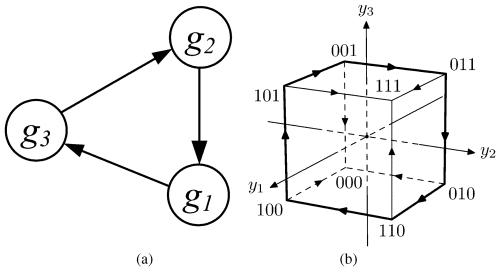

Fig. 12. A wiring scheme with a positive circuit and the unique Boolean Glass network complying to it. (a) Wiring diagram. (b) Boolean Glass network.

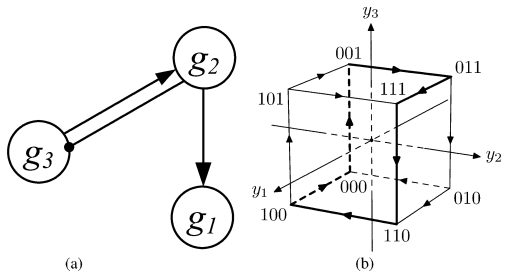

Fig. 13. A wiring scheme and the unique Boolean Glass network complying to it. (a) Wiring diagram. (b) Boolean Glass network.

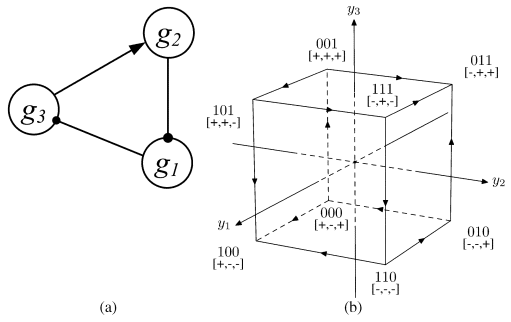

Fig. 14. A sample Glass model corresponding to a given wiring scheme. (a) A wiring diagram. (b) Boolean Glass network (focal points' signs are in brackets).

L denote the length of the cycle, i.e., the number of the nodes of this cycle. Let $\boldsymbol{f}^{+} = (\boldsymbol{f}^{+(1)}, \ldots, \boldsymbol{f}^{+(L)})$ be a sequence of unknown absolute values of the focal coordinates $\boldsymbol{f}^{(k)}$ and let $s = (sign(f_i^{(1)}), \ldots, sign(f_i^{(L)}))$ be the sequence of the signs of the coordinates defined by the given diagram. Based on the criteria given in [15], we introduce the following set of equalities and inequalities that are satisfied iff a periodic flow exists.

1) Let $\boldsymbol{y}(k)$ denote the coordinate vector of a phase trajectory when it crosses the face of the orthant that corresponds to the hypercube edge connecting nodes k and $k+1$. The coordinates are calculated iteratively [15]

$$y_i^{(k+1)} = \frac{f_i^{(k)} y_j^{(k)} - f_j^{(k)}}{y_j^{(k)} - f_j^{(k)}} \tag{3}$$

where j indicates the variable that is switching on the exit boundary for this orthant (i.e., $y_j^{(k+1)} = 0$).

2) The faces of the orthant crossed by the flow along the cycle are specified by

$$y_j^{(k)} = 0; \quad O^{(k)} \tilde{\boldsymbol{y}}^{(k)} > 0 \tag{4}$$

where $\tilde{\boldsymbol{y}}^{(k)}$ is the vector $\boldsymbol{y}^{(k)}$ without coordinate $y_j^{(k)}$, and $O^{(k)}$ is the $(n-1) \times (n-1)$ diagonal matrix defining the signs of the coordinates on the face of the orthant with $O_{ii}^{(k)} = \pm 1$. The system of inequalities written for all k is equivalent to the *returning cone* condition [15] that ensures flow along the nodes of the cycle.

3) Following the notation of [15], let A denote the matrix that is associated with the Poincaré map on the starting face of the orthant that is specified by the first node of the hypercube cycle. If the Glass PLDE has a periodic orbit along the cycle, the staring point $\boldsymbol{y}^{(1)}$ is a fixed point of the Poincaré map and is computed as follows:

$$\boldsymbol{y}^{(1)} = \frac{(\lambda - 1)v}{\langle \phi, v \rangle} \tag{5}$$

where λ and v is the eigenvalue and the eigenvector of A, respectively, and the elements of the matrix A and the vector ϕ can be analytically calculated as functions of $\boldsymbol{f}^{+}$ for any given sign sequence s [15].

4) The eigenvalue has to be real and greater than unity

$$\lambda > 1. \tag{6}$$

The additional condition that λ is the dominant eigenvalue guarantees asymptotic stability of the orbit.

The equalities and inequalities (3)–(6) can be seen as a system of constraints on the set of $n \cdot L$ unknown parameters $f_i^{+(k)}$, and of $n-1$ coordinates $\tilde{y}_i^{(1)}$ of the fixed point. For example, the inequality (6) does not require the computation of the eigenvalue but serves as a constraint on the coefficients of the characteristic polynomial $|A - \lambda E| = 0$. If the system (3)–(6) is consistent, there is a Glass PLDE that possesses a periodic orbit, and any valuation of $\boldsymbol{f}^{+}, \tilde{\boldsymbol{y}}^{(1)}$ satisfying the system defines both the Glass PLDE and the initial conditions of the periodic orbit.

B. Experimental Results

We have conducted an experimental evaluation of the method suggested above, utilizing the results of our classification of the three-dimensional Glass PLDE with 1-period orbits. The search for an instance satisfying the system (3)–(6) was implemented in Mathematica utilizing the subroutines for cylindrical decomposition. The identification of the PLDE with periodic orbits was carried out for three transition diagrams with the cycles of length six shown in Figs. 11–13, respectively. Due to memory restrictions of the machine used, the search was conducted only with two unknown focal coordinates. The absolute values of all other focal coordinates were fixed and of equal unity. Thus, the synthesis of the PLDE was limited to the simultaneous perturbation of two focal coordinates of a Boolean Glass network that was defined by the given transition diagram. During the search, we

TABLE VIII
ALL POSSIBLE CONFIGURATIONS

L	#equilibria	#complex cycles	#cubes
4	0	1	29
	1	0	2
	1	1	43
	1	2	3
	2	0	1
	2	1	3
6	0	1	29
	1	0	2
	1	1	43
	1	2	3
	2	0	1
	2	1	3
8	0	1	29
	1	1	37
	1	2	3
10	0	1	29
	1	1	4
12	0	1	18
	1	1	8
14	0	1	29
	1	1	4
16	0	1	22
	1	1	4
18	0	1	19
	1	1	4
20	0	1	20
	1	1	4
22	0	1	12
	1	1	4
24	0	1	12
26	0	1	4

checked all 153 possible combinations of two perturbed coordinates, out of 18 focal coordinates of the nodes of the cycles.

In the first two cases, the search resulted in 12 Glass PLDE with periodic orbits, and in the third case (see Fig. 13), a total of 11 such networks were identified. Tables IX–XI in the Appendix C list the focal points of the PLDE and the initial conditions of the periodic orbits we found. Our results indicate that the perturbation of two coordinates in other than the listed cases cannot produce periodic orbits. In the third case, four of 11 periodic orbits appeared to be asymptotically stable. In the first two cases, all orbits found are asymptotically unstable, and the results show that no stable orbits can be constructed by any two-coordinate perturbation of the given Boolean PLDE. Note that existence of a stable periodic orbit in the first or in the second case would have contradicted the conjecture about stable periodic solutions, as both the first and the second wiring schemes are the positive circuits.

VI. CONCLUSION AND FUTURE WORK

The Glass PLDE model is frequently used as an approximate model in Systems Biology. The dynamics of Glass PLDE can be formalized as paths through multi-dimensional binary hypercubes. The dynamics of interest in Systems Biology correspond to binary codes that are well studied in the information theory literature, e.g., to snake-in-the-box codes or specific circuit codes.

This paper reports results on the dynamics of Glass PLDE that were obtained by means of classifications of the codes that correspond to the Glass PLDE. We have introduced two new classes of complex attracting sets for the Glass PLDE, and have defined the corresponding cyclic codes. We have also suggested a classification of the dynamics in Glass networks with respect to their wiring schemes, which are a standard model for the interaction among genes. By means of a reduction of the search for the codes to a propositional SAT instance, we have obtained a full classification of the cyclic attractors up to dimension six for wiring schemes with three genes and three interactions.

The paper also suggests a method for constructing the Glass transition diagrams for a given wiring scheme. We have applied this technique to a gene network regulating the cell division of fission yeast. An algebraic method of the construction of the Glass PLDE with periodic orbits along given cycles of the transition diagrams was proposed and tested. We conclude that results on hypercube paths can contribute to the understanding of the complex dynamics of biological systems.

Future Work

Impact of these observations in Systems Biology is hindered by the fact that biological systems can easily contain hundreds of genes; however, an exhaustive enumeration of the corresponding circuit codes is clearly infeasible. We therefore propose to investigate the implications of analytical results on cyclic codes on the corresponding Glass PLDE.

APPENDIX A
A PROPOSITIONAL SAT ENCODING FOR CYCLES ADHERING TO WIRING DIAGRAMS

1) From Interaction Graphs to Glass Models: Let us consider a sample wiring scheme presented in Fig. 14(a), in which first gene is suppressed by the second $g_2 \dashv g_1$ and is suppressing the third $g_1 \dashv g_2$. The only activating edge in this scheme is that of $g_3 \rightarrow g_2$. In what follows, we show that the Boolean Glass network presented in Fig. 14(b) respects that wiring scheme.

First, let us define signs of focal points for each orthant. For an equilibrium point, like 100 or 011 in the figure, the signs coincide with that of the orthant; otherwise, the rule is to invert the sign if there is a possible flow along that direction (see signs in brackets in Fig. 14(b)). In other words, focal point at a given orthant is obtained by summing up the outgoing vectors.

Then, a given edge in the cube does not violate the scheme if changes in signs of orthant and focal point comply to a given wiring scheme. For instance, consider the edge $000 \rightarrow 100$ enabling the first gene. The focal point of the target node differs only in the third position. Its decrease indicates that the first gene suppresses the third because the signs of orthants and focal points change are different. If the wiring scheme in Fig. 14(a) had no edge $g_1 \dashv g_3$, such behaviour would be depricated.

The rest of this section provides details of our SAT encoding of hypercubes compliant to a given wiring scheme.

2) SAT Encoding: Let us begin by introducing $(2^n \cdot n)$ Boolean variables that mimic coordinates of hypercube nodes: the variable $\tilde{x}_i[j]$, where $0 \leq i < 2^n$ and $0 \leq j < n$, denotes the jth bit in the binary representation of node i and is valuated correspondingly (in advance).

In our setting, the hypercube is fully connected, i.e., all $(n \cdot 2^{n-1})$ edges are present. Thus, there are $(n \cdot 2^{n-1})$ variables

TABLE IX
PERIODIC ORBITS WITH WS: $1 \longrightarrow 2 \dashrightarrow 3 \dashrightarrow 1$; FOCAL POINTS ALONG CYCLE IN TRANSITION DIAGRAM OF INITIAL BOOLEAN GLASS PLDE $f_i^{(k)} = ((1,-1,1),(1,1,1),(1,1,-1),(-1,1,-1),(-1,-1,-1),(-1,-1,1))$, SHOWN FIXED POINT IS LOCATED ON ORTHANT FACE $y_1^* < 0; y_2^* = 0; y_3^* < 0$

perturbed focal coordinate: 1	2	fixed point coordinate y_1^*	y_3^*
$f_2^{(1)} = -20$	$f_1^{(2)} = \frac{5}{128}$	$\frac{(-1+\frac{1}{5}(1082-2\sqrt{289481}))\left(\frac{381}{256}+\frac{-1082+2\sqrt{289481}}{1024}\right)}{\frac{607}{5}-\frac{512}{5}\left(\frac{381}{256}+\frac{-1082+2\sqrt{289481}}{1024}\right)}$	$\frac{-1+\frac{1}{5}(1082-2\sqrt{289481})}{\frac{607}{5}-\frac{512}{5}\left(\frac{381}{256}+\frac{-1082+2\sqrt{289481}}{1024}\right)}$
$f_2^{(1)} = -128$	$f_3^{(2)} = \frac{11}{12}$	$\frac{(-1+\frac{1}{4}(1351-\sqrt{1813937}))(\frac{1323}{43}+\frac{1}{86}(-1351+\sqrt{1813937}))}{140-13(\frac{1323}{43}+\frac{1}{86}(-1351+\sqrt{1813937}))}$	$\frac{-1+\frac{1}{4}(1351-\sqrt{1813937})}{140-13(\frac{1323}{43}+\frac{1}{86}(-1351+\sqrt{1813937}))}$
$f_2^{(1)} = -\frac{11}{2}$	$f_1^{(6)} = -128$	$\frac{(-1+\frac{1}{4}(1351-\sqrt{1813937}))(\frac{71}{16}+\frac{1}{32}(-1351+\sqrt{1813937}))}{\frac{17}{2}-4(\frac{71}{16}+\frac{1}{32}(-1351+\sqrt{1813937}))}$	$\frac{-1+\frac{1}{4}(1351-\sqrt{1813937})}{\frac{17}{2}-4(\frac{71}{16}+\frac{1}{32}(-1351+\sqrt{1813937}))}$
$f_3^{(1)} = \frac{1}{32}$	$f_1^{(6)} = -16$	$\frac{(247-8\sqrt{953})(52+\frac{1}{8}(-248+8\sqrt{953}))}{128-4(52+\frac{1}{8}(-248+8\sqrt{953}))}$	$\frac{247-8\sqrt{953}}{128-4(52+\frac{1}{8}(-248+8\sqrt{953}))}$
$f_3^{(2)} = 128$	$f_1^{(3)} = \frac{11}{12}$	$\frac{(-1+\frac{1}{4}(1351-\sqrt{1813937}))\left(\frac{206}{199}+\frac{-1351+\sqrt{1813937}}{1592}\right)}{258-258\left(\frac{206}{199}+\frac{-1351+\sqrt{1813937}}{1592}\right)}$	$\frac{-1+\frac{1}{4}(1351-\sqrt{1813937})}{258-258\left(\frac{206}{199}+\frac{-1351+\sqrt{1813937}}{1592}\right)}$
$f_3^{(2)} = 20$	$f_2^{(3)} = \frac{5}{128}$	$\frac{(-1+\frac{1}{5}(1082-2\sqrt{289481}))(\frac{79}{47}+\frac{1}{940}(-1082+2\sqrt{289481}))}{\frac{456}{5}-\frac{333}{5}(\frac{79}{47}+\frac{1}{940}(-1082+2\sqrt{289481}))}$	$\frac{-1+\frac{1}{5}(1082-2\sqrt{289481})}{\frac{456}{5}-\frac{333}{5}(\frac{79}{47}+\frac{1}{940}(-1082+2\sqrt{289481}))}$
$f_1^{(3)} = 128$	$f_2^{(4)} = -\frac{11}{2}$	$\frac{(-1+\frac{1}{4}(1351-\sqrt{1813937}))\left(\frac{1069}{542}+\frac{-1351+\sqrt{1813937}}{1084}\right)}{\frac{35}{2}-13\left(\frac{1069}{542}+\frac{-1351+\sqrt{1813937}}{1084}\right)}$	$\frac{-1+\frac{1}{4}(1351-\sqrt{1813937})}{\frac{35}{2}-13\left(\frac{1069}{542}+\frac{-1351+\sqrt{1813937}}{1084}\right)}$
$f_1^{(3)} = 20$	$f_3^{(4)} = -\frac{5}{128}$	$\frac{(-1+\frac{1}{5}(1082-2\sqrt{289481}))(\frac{194}{121}+\frac{1}{968}(-1082+2\sqrt{289481}))}{\frac{758}{5}-\frac{512}{5}(\frac{194}{121}+\frac{1}{968}(-1082+2\sqrt{289481}))}$	$\frac{-1+\frac{1}{5}(1082-2\sqrt{289481})}{\frac{758}{5}-\frac{512}{5}(\frac{194}{121}+\frac{1}{968}(-1082+2\sqrt{289481}))}$
$f_2^{(4)} = 20$	$f_1^{(5)} = -\frac{5}{128}$	$\frac{(-1+\frac{1}{5}(1082-2\sqrt{289481}))(\frac{395}{242}+\frac{1}{968}(-1082+2\sqrt{289481}))}{61-42(\frac{395}{242}+\frac{1}{968}(-1082+2\sqrt{289481}))}$	$\frac{-1+\frac{1}{5}(1082-2\sqrt{289481})}{61-42(\frac{395}{242}+\frac{1}{968}(-1082+2\sqrt{289481}))}$
$f_2^{(4)} = 128$	$f_3^{(5)} = -\frac{11}{2}$	$\frac{(-1+\frac{1}{4}(1351-\sqrt{1813937}))\left(\frac{833}{551}+\frac{-1351+\sqrt{1813937}}{1102}\right)}{385-258\left(\frac{833}{551}+\frac{-1351+\sqrt{1813937}}{1102}\right)}$	$\frac{-1+\frac{1}{4}(1351-\sqrt{1813937})}{385-258\left(\frac{833}{551}+\frac{-1351+\sqrt{1813937}}{1102}\right)}$
$f_3^{(5)} = -128$	$f_1^{(6)} = -\frac{11}{2}$	$\frac{(-1+\frac{1}{4}(1351-\sqrt{1813937}))\left(\frac{648}{389}+\frac{-1351+\sqrt{1813937}}{1556}\right)}{4-4\left(\frac{648}{389}+\frac{-1351+\sqrt{1813937}}{1556}\right)}$	$\frac{-1+\frac{1}{4}(1351-\sqrt{1813937})}{4-4\left(\frac{648}{389}+\frac{-1351+\sqrt{1813937}}{1556}\right)}$
$f_3^{(5)} = -20$	$f_2^{(6)} = -\frac{5}{128}$	$\frac{(-1+\frac{1}{5}(1082-2\sqrt{289481}))(\frac{381}{235}+\frac{1}{940}(-1082+2\sqrt{289481}))}{\frac{1004}{5}-127(\frac{381}{235}+\frac{1}{940}(-1082+2\sqrt{289481}))}$	$\frac{-1+\frac{1}{5}(1082-2\sqrt{289481})}{\frac{1004}{5}-127(\frac{381}{235}+\frac{1}{940}(-1082+2\sqrt{289481}))}$

representing edges. A variable for an edge (a,b) is denoted as $\tilde{e}(a,b)$.

3) Encoding Focal Points: Since every orthant has a focal point associated with it, the number of Boolean variables we need for the focal points is the same as the number of cube nodes: $\tilde{f}_i[j]$, where $0 \le i < 2^n$ and $0 \le j < n$. Indeed, for every hypercube node we have to store the sign of its focal point w.r.t. every dimension. For every edge of the cube, the following constraint should be met

$$\tilde{e}(a,b) \Rightarrow \left(\tilde{f}_a[k] \Leftrightarrow \tilde{f}_b[k] \Leftrightarrow \tilde{x}_b[k]\right)$$
$$\neg\tilde{e}(a,b) \Rightarrow \left(\tilde{f}_a[k] \Leftrightarrow \tilde{f}_b[k] \Leftrightarrow \tilde{x}_a[k]\right)$$

where b is the node adjacent to a along kth axis: $b = a^{neigh(k)}$, i.e., the coordinates of a and b differ only in kth bit.

4) The Interaction Graph: The encoding of an interaction graph W is done by following the adjacency matrix and requires $4{\cdot}|E(K_n)|$ variables (where K_n denotes an undirected complete graph). The number of edges of a complete graph over n nodes has to be doubled because we need two kinds of edges: activating and suppressing. $\tilde{W}act_{p,r}$ and $\tilde{W}sup_{p,r}$, $0 \le p,r < n$, directly mimic the provided interactions:

$$\bigwedge_{p=0}^{n-1}\bigwedge_{r=0,r\neq p}^{n-1}\begin{cases}\tilde{W}act_{p,r} & \text{if } p \longrightarrow r \in W\\ \neg\tilde{W}act_{p,r} & \text{if } p \longrightarrow r \notin W\\ \tilde{W}sup_{p,r} & \text{if } p \dashrightarrow r \in W\\ \neg\tilde{W}sup_{p,r} & \text{if } p \dashrightarrow r \notin W\end{cases}. \quad (7)$$

5) Compliance: For each edge of the n-cube the compliance of changes in signs of coordinates and foci with the given interaction graph is desired. That is, if the signs are opposite, the wiring scheme has to contain the inhibiting edge and if they are the same—the activating edge. As first step, we encode the signs. For an edge (a,b), $b = a^{neigh(k)}$, and axes $m \neq k$, $0 \le m < n$

$$\tilde{x}^k_{\text{inc}} \Leftrightarrow \neg\tilde{x}_a[k] \wedge \tilde{x}_b[k] \quad (8)$$
$$\tilde{x}^k_{\text{dec}} \Leftrightarrow \neg\tilde{x}^k_{\text{inc}} \quad (9)$$
$$\tilde{f}^m_{\text{inc}} \Leftrightarrow \neg\tilde{f}_a[m] \wedge \tilde{x}_b[m] \quad (10)$$
$$\tilde{f}^m_{\text{dec}} \Leftrightarrow \tilde{f}_a[m] \wedge \neg\tilde{f}_b[m]. \quad (11)$$

Note that for many combinations of k and m (10) and (11) are not triggered since the signs of focal points stay the same during traversal (for the above example, a single focal point changes its sign for every traversal of a hypercube edge, see Table VI).

Then, activation and suppression predicates are enabled if the signs of coordinates and focal points change accordingly

$$\tilde{act}^{k,m}(a,b) \Leftrightarrow \left(\left(\tilde{x}^k_{\text{inc}} \wedge \tilde{f}^m_{\text{inc}}\right) \vee \left(\tilde{x}^k_{\text{dec}} \wedge \tilde{f}^m_{\text{dec}}\right)\right) \quad (12)$$
$$\tilde{\text{sup}}^{k,m}(a,b) \Leftrightarrow \left(\left(\tilde{x}^k_{\text{inc}} \wedge \tilde{f}^m_{\text{dec}}\right) \vee \left(\tilde{x}^k_{\text{dec}} \wedge \tilde{f}^m_{\text{inc}}\right)\right). \quad (13)$$

Here, $\tilde{\text{act}}^{k,m}(a,b)$ indicates activation behavior between genes k and m, which takes place if a change in the coordinate along axis k has the same sign as the change in the focal point along axis m. Similarly, the rules for suppression are modeled by (13). The cube in Fig. 14 has a cyclic attractor, thus the phase flow is unambiguous, and therefore each hypercube edge infers one gene interaction only (see last column in Table VI).

TABLE X

PERIODIC ORBITS WITH WS: $1 \longrightarrow 2 \longrightarrow 3 \longrightarrow 1$; FOCAL POINTS ALONG CYCLE IN TRANSITION DIAGRAM OF INITIAL BOOLEAN GLASS PLDE $f_i^{(k)} = ((-1,1,1),(-1,1,-1),(1,1,-1),(1,-1,-1),(1,-1,1),(-1,-1,1))$, SHOWN FIXED POINT IS LOCATED ON ORTHANT FACE $y_1^* > 0; y_2^* < 0; y_3^* = 0$

perturbed focal coordinate: 1	2	fixed point coordinate y_1^*	y_2^*
$f_1^{(1)} = -\frac{1}{32}$	$f_2^{(6)} = -16$	$\frac{(247-8\sqrt{953})\left(-\frac{5}{256}+\frac{248-8\sqrt{953}}{4096}\right)}{-4-128\left(-\frac{5}{256}+\frac{248-8\sqrt{953}}{4096}\right)}$	$\frac{247-8\sqrt{953}}{-4-128\left(-\frac{5}{256}+\frac{248-8\sqrt{953}}{4096}\right)}$
$f_3^{(1)} = 128$	$f_1^{(2)} = -\frac{11}{2}$	$\frac{\left(-\frac{7}{199}+\frac{1351-\sqrt{1813937}}{1592}\right)\left(-1+\frac{1}{4}(1351-\sqrt{1813937})\right)}{-13-140\left(-\frac{7}{199}+\frac{1351-\sqrt{1813937}}{1592}\right)}$	$\frac{-1+\frac{1}{4}(1351-\sqrt{1813937})}{-13-140\left(-\frac{7}{199}+\frac{1351-\sqrt{1813937}}{1592}\right)}$
$f_3^{(1)} = 20$	$f_2^{(2)} = \frac{5}{128}$	$\frac{\left(-\frac{32}{47}+\frac{1}{940}(1082-2\sqrt{289481})\right)\left(-1+\frac{1}{5}(1082-2\sqrt{289481})\right)}{-\frac{512}{5}-\frac{607}{5}\left(-\frac{32}{47}+\frac{1}{940}(1082-2\sqrt{289481})\right)}$	$\frac{-1+\frac{1}{5}(1082-2\sqrt{289481})}{-\frac{512}{5}-\frac{607}{5}\left(-\frac{32}{47}+\frac{1}{940}(1082-2\sqrt{289481})\right)}$
$f_3^{(1)} = \frac{11}{2}$	$f_2^{(6)} = -128$	$\frac{\left(-\frac{10}{43}+\frac{1351-\sqrt{1813937}}{11008}\right)\left(-1+\frac{1}{4}(1351-\sqrt{1813937})\right)}{-4-\frac{17}{2}\left(-\frac{10}{43}+\frac{1351-\sqrt{1813937}}{11008}\right)}$	$\frac{-1+\frac{1}{4}(1351-\sqrt{1813937})}{-4-\frac{17}{2}\left(-\frac{10}{43}+\frac{1351-\sqrt{1813937}}{11008}\right)}$
$f_1^{(2)} = -128$	$f_2^{(3)} = \frac{11}{2}$	$\frac{\left(-\frac{527}{542}+\frac{1351-\sqrt{1813937}}{1084}\right)\left(-1+\frac{1}{4}(1351-\sqrt{1813937})\right)}{-258-258\left(-\frac{527}{542}+\frac{1351-\sqrt{1813937}}{1084}\right)}$	$\frac{-1+\frac{1}{4}(1351-\sqrt{1813937})}{-258-258\left(-\frac{527}{542}+\frac{1351-\sqrt{1813937}}{1084}\right)}$
$f_1^{(2)} = -20$	$f_3^{(3)} = -\frac{5}{128}$	$\frac{\left(-\frac{73}{121}+\frac{1}{968}(1082-2\sqrt{289481})\right)\left(-1+\frac{1}{5}(1082-2\sqrt{289481})\right)}{-\frac{333}{5}-\frac{456}{5}\left(-\frac{73}{121}+\frac{1}{968}(1082-2\sqrt{289481})\right)}$	$\frac{-1+\frac{1}{5}(1082-2\sqrt{289481})}{-\frac{333}{5}-\frac{456}{5}\left(-\frac{73}{121}+\frac{1}{968}(1082-2\sqrt{289481})\right)}$
$f_2^{(3)} = 20$	$f_1^{(4)} = \frac{5}{128}$	$\frac{\left(-\frac{153}{242}+\frac{1}{968}(1082-2\sqrt{289481})\right)\left(-1+\frac{1}{5}(1082-2\sqrt{289481})\right)}{-\frac{512}{5}-\frac{758}{5}\left(-\frac{153}{242}+\frac{1}{968}(1082-2\sqrt{289481})\right)}$	$\frac{-1+\frac{1}{5}(1082-2\sqrt{289481})}{-\frac{512}{5}-\frac{758}{5}\left(-\frac{153}{242}+\frac{1}{968}(1082-2\sqrt{289481})\right)}$
$f_2^{(3)} = 128$	$f_3^{(4)} = -\frac{11}{2}$	$\frac{\left(-\frac{282}{551}+\frac{1351-\sqrt{1813937}}{1102}\right)\left(-1+\frac{1}{4}(1351-\sqrt{1813937})\right)}{-13-\frac{35}{2}\left(-\frac{282}{551}+\frac{1351-\sqrt{1813937}}{1102}\right)}$	$\frac{-1+\frac{1}{4}(1351-\sqrt{1813937})}{-13-\frac{35}{2}\left(-\frac{282}{551}+\frac{1351-\sqrt{1813937}}{1102}\right)}$
$f_1^{(4)} = 128$	$f_1^{(6)} = -\frac{11}{2}$	$\frac{\left(-\frac{66}{131}+\frac{2}{131}(229-\sqrt{52433})\right)\left(-1+\frac{1}{32}(229-\sqrt{52433})\right)}{-\frac{1}{32}+\frac{125}{64}\left(-\frac{66}{131}+\frac{2}{131}(229-\sqrt{52433})\right)}$	$\frac{-1+\frac{1}{32}(229-\sqrt{52433})}{-\frac{1}{32}+\frac{125}{64}\left(-\frac{66}{131}+\frac{2}{131}(229-\sqrt{52433})\right)}$
$f_1^{(4)} = 20$	$f_2^{(6)} = -\frac{5}{128}$	$\frac{\left(-1+\frac{1}{640}(1439-\sqrt{2069921})\right)\left(-\frac{12}{23}+\frac{2}{115}(1439-\sqrt{2069921})\right)}{-\frac{1}{5}+\frac{17}{10}\left(-\frac{12}{23}+\frac{2}{115}(1439-\sqrt{2069921})\right)}$	$\frac{-1+\frac{1}{640}(1439-\sqrt{2069921})}{-\frac{1}{5}+\frac{17}{10}\left(-\frac{12}{23}+\frac{2}{115}(1439-\sqrt{2069921})\right)}$
$f_1^{(5)} = 128$	$f_2^{(6)} = -\frac{11}{2}$	$\frac{\left(-\frac{5}{8}+\frac{1}{176}(1351-\sqrt{1813937})\right)\left(-1+\frac{1}{4}(1351-\sqrt{1813937})\right)}{-4-4\left(-\frac{5}{8}+\frac{1}{176}(1351-\sqrt{1813937})\right)}$	$\frac{-1+\frac{1}{4}(1351-\sqrt{1813937})}{-4-4\left(-\frac{5}{8}+\frac{1}{176}(1351-\sqrt{1813937})\right)}$
$f_1^{(5)} = 20$	$f_3^{(6)} = \frac{5}{128}$	$\frac{\left(-\frac{5}{8}+\frac{1082-2\sqrt{289481}}{1024}\right)\left(-1+\frac{1}{5}(1082-2\sqrt{289481})\right)}{-127-\frac{1004}{5}\left(-\frac{5}{8}+\frac{1082-2\sqrt{289481}}{1024}\right)}$	$\frac{-1+\frac{1}{5}(1082-2\sqrt{289481})}{-127-\frac{1004}{5}\left(-\frac{5}{8}+\frac{1082-2\sqrt{289481}}{1024}\right)}$

TABLE XI

PERIODIC ORBITS WITH WS: $2 \multimap 1 \longrightarrow 2 \longrightarrow 3$; FOCAL POINTS ALONG CYCLE IN TRANSITION DIAGRAM OF INITIAL BOOLEAN GLASS PLDE $f_i^{(k)} = ((-1,-1,1),(-1,1,1),(1,1,-1),(1,1,-1),(1,-1,-1),(-1,-1,1))$, SHOWN FIXED POINT IS LOCATED ON ORTHANT FACE $y_1^* = 0; y_2^* < 0; y_3^* < 0$

perturbed focal coordinate: 1	2	fixed point coordinate y_2^*	y_3^*
$f_1^{(2)} = -\frac{25}{32}$	$f_3^{(5)} = -\frac{5}{4}$	$-\frac{7}{135}$	$-\frac{1}{135}$ Stable
$f_1^{(2)} = -\frac{1}{4}$	$f_3^{(6)} = -\frac{3}{32}$	$\frac{\left(-1+\frac{1}{256}(343-\sqrt{52113})\right)\left(-\frac{119}{107}+\frac{1}{214}(343-\sqrt{52113})\right)}{-\frac{19}{4}-\frac{19}{4}\left(-\frac{119}{107}+\frac{1}{214}(343-\sqrt{52113})\right)}$	$\frac{-1+\frac{1}{256}(343-\sqrt{52113})}{-\frac{19}{4}-\frac{19}{4}\left(-\frac{119}{107}+\frac{1}{214}(343-\sqrt{52113})\right)}$
$f_3^{(2)} = \frac{5}{4}$	$f_1^{(5)} = \frac{25}{32}$	$-\frac{29}{605}$	$-\frac{3}{605}$ Stable
$f_3^{(2)} = \frac{13}{8}$	$f_3^{(5)} = -\frac{3}{2}$	$-\frac{5}{26}$	$-\frac{3}{104}$ Stable
$f_3^{(2)} = \frac{5}{4}$	$f_3^{(6)} = \frac{3}{4}$	$\frac{\left(-1+\frac{1}{16}(19-\sqrt{41})\right)\left(-7+\frac{1}{2}(19-\sqrt{41})\right)}{-5-5\left(-7+\frac{1}{2}(19-\sqrt{41})\right)}$	$\frac{-1+\frac{1}{16}(19-\sqrt{41})}{-5-5\left(-7+\frac{1}{2}(19-\sqrt{41})\right)}$
$f_1^{(3)} = \frac{13}{8}$	$f_3^{(5)} = -2$	$-\frac{5}{41}$	$-\frac{4}{41}$ Stable
$f_1^{(3)} = \frac{5}{4}$	$f_3^{(6)} = \frac{3}{4}$	$\frac{\left(-1+\frac{1}{20}(19-\sqrt{41})\right)\left(-7+\frac{1}{2}(19-\sqrt{41})\right)}{-\frac{22}{5}-\frac{21}{5}\left(-7+\frac{1}{2}(19-\sqrt{41})\right)}$	$\frac{-1+\frac{1}{20}(19-\sqrt{41})}{-\frac{22}{5}-\frac{21}{5}\left(-7+\frac{1}{2}(19-\sqrt{41})\right)}$
$f_3^{(3)} = -\frac{3}{32}$	$f_1^{(5)} = \frac{1}{4}$	$\frac{\left(-1+\frac{1}{256}(343-\sqrt{52113})\right)\left(-\frac{166}{67}+\frac{1}{134}(343-\sqrt{52113})\right)}{-\frac{585}{64}-\frac{793}{128}\left(-\frac{166}{67}+\frac{1}{134}(343-\sqrt{52113})\right)}$	$\frac{-1+\frac{1}{256}(343-\sqrt{52113})}{-\frac{585}{64}-\frac{793}{128}\left(-\frac{166}{67}+\frac{1}{134}(343-\sqrt{52113})\right)}$
$f_3^{(3)} = -\frac{3}{4}$	$f_3^{(5)} = -\frac{5}{4}$	$\frac{(5-\sqrt{41})\left(-1+\frac{1}{16}(19-\sqrt{41})\right)}{-6-5(5-\sqrt{41})}$	$\frac{-1+\frac{1}{16}(19-\sqrt{41})}{-6-5(5-\sqrt{41})}$
$f_3^{(3)} = -\frac{3}{4}$	$f_1^{(6)} = -\frac{5}{4}$	$\frac{(5-\sqrt{41})\left(-1+\frac{1}{20}(19-\sqrt{41})\right)}{-\frac{29}{5}-\frac{47}{10}(5-\sqrt{41})}$	$\frac{-1+\frac{1}{20}(19-\sqrt{41})}{-\frac{29}{5}-\frac{47}{10}(5-\sqrt{41})}$
$f_3^{(3)} = -\frac{3}{32}$	$f_3^{(6)} = \frac{1}{8}$	$\frac{\left(-\frac{302}{199}+\frac{1}{199}(331-3\sqrt{10353})\right)\left(-1+\frac{1}{128}(331-3\sqrt{10353})\right)}{-\frac{45}{4}-\frac{61}{8}\left(-\frac{302}{199}+\frac{1}{199}(331-3\sqrt{10353})\right)}$	$\frac{-1+\frac{1}{128}(331-3\sqrt{10353})}{-\frac{45}{4}-\frac{61}{8}\left(-\frac{302}{199}+\frac{1}{199}(331-3\sqrt{10353})\right)}$

Finally, we restrict activating and suppressing behavior to take place only if allowed by the corresponding edge of the interaction graph

$$\tilde{e}(a,b) \wedge \tilde{\text{act}}^{k,m}(a,b) \Longrightarrow \tilde{W}\text{act}_{k,m} \tag{14}$$

$$\tilde{e}(a,b) \wedge \tilde{\text{sup}}^{k,m}(a,b) \Longrightarrow \tilde{W}\sup_{k,m}. \tag{15}$$

6) Completeness: The formulae (14) and (15) specify compliance of a hypercube traversals to a given interaction graph. Hovewer, one needs to specify that every edge of a wiring scheme is supported by some edge of the hypercube, what we call *completeness*. In order to specify completeness, it has to be asserted that at least one of the implications in (14) or (15) is triggered:

$$\tilde{W}\text{act}_{k,m} \Longrightarrow \bigvee_{a=0}^{2^n-1} \tilde{e}(a, a^{neigh(k)}) \wedge \tilde{\text{act}}^{k,m}(a, a^{neigh(k)})$$

$$\tilde{W}\sup_{k,m} \Longrightarrow \bigvee_{a=0}^{2^n-1} \tilde{e}(a, a^{neigh(k)}) \wedge \tilde{\text{sup}}^{k,m}(a, a^{neigh(k)}).$$

A satisfying assignment to a conjunction of the above formulae provides us a desired Glass model. All models can be listed using a specialized ALL-SAT solver, or by appending blocking clauses for every solution found until UNSAT is reached.

Appendix B
Classification of Wiring Schemes With Three Edges

(See Table VII.)

Appendix C
Glass Models With Periodic Orbits Corresponding Fig. 9

Table VIII presents results of the run of our algorithm on cubes complying to the scheme in Fig. 9 for all lengths of cycles from 4 to 32. We have obtained *all* such cubes within 16 h.

Acknowledgment

The authors would like to thank Jasmin Fisher for stimulating discussions about gene regulatory networks; in particular, in connection with the application to *C. elegans*.

References

[1] I. Zinovik, D. Kroening, and Y. Chebiryak, "An algebraic algorithm for the identification of Glass networks with periodic orbits along cyclic attractors," in *Proc. Algebraic Biol. Second Int. Conf. AB 2007*, 2007, vol. 4545, Lecture Notes in Computer Science, pp. 140–154.

[2] Y. Chebiryak, T. Wahl, D. Kroening, and L. Haller, O. Kullmann, Ed., "Finding lean induced cycles in binary hypercubes," in *Proc. Theory Applicat. Satisfiability Testing – SAT 2009*, 2009, vol. 5584, LNCS, pp. 18–31.

[3] H. de Jong, "Modeling and simulation of genetic regulatory systems: A literature review," *J. Comp. Biol.*, vol. 9, no. 1, pp. 67–103, 2002.

[4] J. Gebert, N. Radde, and G. Weber, "Modeling gene regulatory networks with piecewise linear differential equations," *European J. Oper. Res.*, vol. 181, no. 3, pp. 1148–1165, 2007.

[5] L. Glass and S. Kauffman, "The logical analysis of continuous non-linear biochemical control networks," *J. Theor. Biol.*, vol. 39, pp. 103–129, 1973.

[6] L. Glass, "Combinatorial aspects of dynamics in biological systems," in *Stat. Mech Stat. Methods in Theory and Application*, U. Landman, Ed. New York: Plenum, 1977, pp. 585–611.

[7] R. Edwards, "Symbolic dynamics and computation in model gene networks," *Chaos*, vol. 11, no. 1, pp. 160–169, 2001.

[8] R. Ghosh, A. Tiwari, and C. Tomlin, "Automated symbolic reachability analysis; with application to delta-notch signalic automata," in *Hybrid Systems: Computation and Control*. Berlin, Germany: Springer, 2003, vol. 2623, Lecture Notes in Computer Science, pp. 233–248.

[9] J. Mason, P. Linsay, J. Collins, and L. Glass, "Evolving complex dynamics in electronic models of genetic networks," *Chaos*, vol. 14, no. 3, pp. 707–715, 2004.

[10] G. Batt, D. Ropers, H. de Jong, J. Geiselmann, R. Mateescu, M. Page, and D. Schneider, "Analysis and verification of qualitative models of genetic regulatory networks: A model-checking approach," in *Proc. 19th Int. Joint Conf. Artif. Intell.*, 2005, pp. 370–375.

[11] T. Gedeon, "Global dynamics of neural nets with infinite gain," *Physica D: Nonlinear Phenomena*, vol. 146, pp. 200–212, 2000.

[12] T. Gedeon, "Attractors in continuous time switching networks," *Commun. Pure Appl. Anal.*, vol. 2, no. 2, pp. 187–209, 2003.

[13] N. Eén and N. Sörensson, "An extensible SAT-solver," in *Theory and Applications of Satisfiability Testing*. Berlin, Germany: Springer, 2004, vol. 2919, Lecture Notes in Computer Science, pp. 502–518.

[14] B. Dutertre and L. de Moura, "A fast linear-arithmetic solver for DPLL(T)," in *Proc. CAV 2006*, 2006, vol. 4144, Lecture Notes in Computer Science, pp. 81–94.

[15] R. Edwards, "Analysis of continuous-time switching networks," *Physica D*, vol. 146, pp. 165–199, 2000.

[16] M. Kaufman, C. Soulé, and R. Thomas, "A new necessary condition on interaction graphs for multistationarity," *J. Theoretic. Biol.*, vol. 248, no. 4, pp. 675–685, 2007.

[17] R. Tanner, "A recursive approach to low complexity codes," *IEEE Trans. Inf. Theory*, vol. 27, pp. 533–547, 1981.

[18] T. Etzion, A. Trachtenberg, and A. Vardy, "Which codes have cycle-free tanner graphs?," *IEEE Trans. Inf. Theory*, vol. 45, pp. 2173–2181, 1999.

[19] R. Edwards and L. Glass, "Combinatorial explosion in model gene networks," *Chaos*, vol. 10, no. 3, pp. 691–704, 2000.

[20] H. de Jong and M. Page, "Search for steady states of piecewise-linear differential equation models of genetic regulatory networks," *IEEE/ACM Trans. Comput. Biol. Bioinform.*, vol. 5, pp. 508–522, 2008.

[21] R. Thomas and M. Kaufman, "Multistationarity, the basis of cell differentiation and memory," *Chaos*, vol. 11, no. 1, pp. 170–195, 2001.

[22] L. Glass and J. Pasternack, "Stable oscillations in mathematical models of biological control systems," *J. Math. Biol.*, vol. 6, pp. 207–223, 1978.

[23] T. Mestl, E. Plahte, and S. Omholt, "Periodic solutions in systems of piecewise-linear differential equations," *Dynam. Stabil. Syst.*, vol. 10, no. 2, pp. 179–193, 1995.

[24] T. Mestl, C. Lemay, and L. Glass, "Chaos in high-dimensional neural and gene networks," *Physica D*, vol. 98, pp. 33–52, 1996.

[25] W. H. Kautz, "Unit distance error checking codes," *IRE Trans. Electron. Comput.*, vol. 7, pp. 179–180, 1958.

[26] R. C. Singleton, "Generalized snake-in-the-box codes," *IEEE Trans. Electron. Comput.*, vol. EC-15, no. 4, pp. 596–602, 1966.

[27] V. Klee, "The use of circuit codes in analog-to-digital conversion," *Graph Theory Its Applicat.*, pp. 121–132, 1970.

[28] S. Kauffman, "A proposal for using the ensemble approach to understand genetic regulatory networks," *Theor. Biol.*, vol. 230, pp. 581–590, 2004.

[29] N. Kam, D. Harel, H. Kugler, R. Marelly, A. Pnueli, E. Hubbard, and M. Stern, "Formal modeling of C. elegans development: A scenario-based approach," in *Proc. First Int. Workshop Computat. Meth. Syst. Biol.*, 2003, vol. 2602, Lecture Notes in Computer Science, pp. 40–20.

[30] L. Glass and J. Pasternack, "Prediction of limit cycles in mathematical models of biological oscillations," *Bull. Math. Biol.*, vol. 40, pp. 27–44, 1978.

[31] Y. Chebiryak and D. Kroening, "Towards a Classification of Hamiltonian Cycles in the 6-Cube," *J. Satisfiability*, vol. 4, pp. 57–74, 2008.

[32] Y. Chebiryak and D. Kroening, "An efficient SAT encoding of circuit codes," in *Proc. IEEE Int. Symp. Inf. Theory Its Applicat.*, Auckland, New Zealand, Dec. 2008, pp. 1235–1238.

[33] I. Zinovik, D. Kroening, and Y. Chebiryak, "Computing binary combinatorial Gray codes via exhaustive search with SAT-solvers," *IEEE Trans. Inf. Theory*, vol. 54, pp. 1819–1823, 2008.

[34] T. Perkinsa, M. Halletta, and L. Glass, "Inferring models of gene expression dynamics," *J. Theoret. Biol.*, vol. 230, pp. 289–299, 2004.

[35] E. Farcot and J.-L. Gouze, "Periodic solutions of piecewise affine gene network models with non uniform decay rates using monotonicity properties," *Acta Biotheoretica*, 2007, to be published.

[36] C. Soulé, "Mathematical approaches to differentiation and gene regulation," *Comptes Rendus-Biologies*, vol. 329, no. 1, pp. 13–20, 2006.

[37] P. Sternberg, "Vulval development," *WormBook*, vol. 1, no. 1, Jun. 2005.

[38] O. Cinquin and J. Demongeot, "Positive and negative feedback: Striking a balance between necessary antagonists," *J. Theoret. Biol.*, vol. 216, no. 2, pp. 229–242, 2002.

[39] B. Novak, Z. Pataki, A. Ciliberto, and J. Tyson, "Mathematical model of the cell division cycle of fission yeast," *Chaos: An Interdiscipl. J. Nonlinear Sci.*, vol. 11, p. 277, 2001.

[40] C. Papadimitriou, *Computational Complexity*. Reading, MA: Addison-Wesley, 1994.

[41] J. Szwarcfiter and P. Lauer, "A search strategy for the elementary cycles of a directed graph," *BIT Numer. Math.*, vol. 16, no. 2, pp. 192–204, 1976.

[42] D. Johnson, "Finding all the elementary circuits of a directed graph," *SIAM J. Comput.*, vol. 4, p. 77, 1975.

[43] R. Tarjan, "Depth-first search and linear graph algorithms," *SIAM J. Comput.*, vol. 1, no. 2, pp. 146–160, 1972.

Igor Zinovik received the M.S. and doctoral degrees in fluid dynamics from Lomonosov Moscow State University, Moscow, Russia, in 1988 and 1992, respectively.

He worked in the Institute of Mechanics at Lomonosov Moscow State University as a Postdoctoral researcher, at the University of Pittsburgh, Pittsburgh, PA, and at the Computer Science Department at the Swiss Technical Institute (ETH), Zürich, Switzerland, as a Research Associate. He is now a Senior Scientist at the Laboratory of Thermodynamics LTNT, Department of Mechanical and Process Engineering at the Swiss Technical Institute (ETH), Zürich. His research interests include computational fluid dynamics, numerical algorithms, and modeling of dynamic systems.

Yury Chebiryak was born in Vladivostok, Russia. He graduated from the Pacific National University, Khabarovsk, Russia, in 2004 and received the M.S. degree in computer science from the University of Saarland, Saarbrücken, Germany, in 2005.

Since 2006, he has been with the Formal Verification group at the Swiss Technical Institute (ETH), Zürich, Switzerland. His research interests include hardware design and verification, SAT-solving, combinatorics, computational biology and hypercubes.

Daniel Kroening received the M.E. and doctoral degrees in computer science from the University of Saarland, Saarbrücken, Germany, in 1999 and 2001, respectively.

He joined the Model Checking group in the Computer Science Department at Carnegie Mellon University, Pittsburgh, PA, in 2001 as a Postdoctoral Researcher. He was an Assistant Professor at the Swiss Technical Institute (ETH), Zürich, Switzerland, from 2004 to 2007. He is now a Reader in the Computing Laboratory at Oxford University, Oxford, U.K. His research interests include automated formal verification, program semantics, and decision procedures.